An Allosteric Synthetic Catalyst: Metal Ions Tune the Activity of an Artificial Phosphodiesterase

Igor O. Fritsky, Reina Ott, Hans Pritzkow, and Roland Krämer*[a]

Abstract: A trinuclear metal complex of general formula $(L{-}H)M_s(M_f)_2$ represents the first allosteric low molecular weight catalyst. L is a polyaza ligand having a tetradentate and two bidentate metal binding sites, M_s is a "structural" (allosteric) metal, and M_f are functional (catalytic) metals which interact with a substrate. In mononuclear $[(L{-}H)M_s]^+$ complexes $[(L{-}H)Cu(MeOH)]ClO_4$ (**1a**), $[(L{-}H)Cu]NO_3 \cdot 2H_2O$ (**1b**), $[(L{-}H)Ni]ClO_4 \cdot 4H_2O$ (**2**), and $[(L{-}H)Pd]ClO_4 \cdot 2H_2O$ (**3**), prepared from L and M^{2+} salts, the metal is strongly bound by an in-plane N_4-coordination (confirmed by X-ray crystal structure determination of **1a**). Formation of trinuclear complexes $[(L{-}H)M_sCu_2]^{5+}$, with two functional Cu^{2+} ions coordinated to the bidentate sites of L, was evidenced in solution by photometric titration and by isolation of $[(L{-}H)Cu_3][PO_4][ClO_4]_2 \cdot 9H_2O$ (**4**). The trinuclear complexes catalyze the cleavage of RNA-analogue 2-(hydroxypropyl)-*p*-nitrophenyl phosphate (HPNP), an activated phosphodiester. From a kinetic analysis of the cleavage rate at various HPNP concentrations, parameters K_{HPNP} (the equilibrium constant for binding of HPNP to $[(L{-}H)M_sCu_2]^{5+}$ and k_{cat} (first-order rate constant for cleavage of HPNP when bound to the catalyst) were derived: $K_M = 170$ ($M_s = Cu^{2+}$), 340 ($M_s = Ni^{2+}$), 2600 ($M_s = Pd^{2+}$) M^{-1}, $k_{cat} = 17 \times 10^{-3}$ ($M_s = Cu^{2+}$), 3.1×10^{-3} ($M_s = Ni^{2+}$), 0.22×10^{-3} ($M_s = Pd^{2+}$) s^{-1}. Obviously, the nature of the allosteric metal ion M_s strongly influences both substrate affinity and reactivity of the catalyst $[(L{-}H)M_sCu_2]^{5+}$. Our interpretation of this observation is that subtle differences in the ionic radius of M_s and in its tendency to distort the $N_4{-}M_s$ coordination plane have a significant influence on the conformation of the catalyst (i.e., preorganization of functional Cu^{2+} ions) and thus on catalytic activity.

Keywords: allosterism · copper · catalysts · enzyme models · phosphodiester cleavage

Introduction

In vivo catalytic activity of enzymes is often controlled by complex regulatory systems. Allosteric regulation is an important possibility for the tuning of catalytic efficiency. An allosteric effector (a molecule or ion) binds in a noncovalent fashion to a site other than the active site but alters the conformation of the enzyme active site. In the active site of *E. coli* alkaline phosphatase a phosphate monoester substrate is hydrolyzed by a dizinc(II) site while a Mg^{2+} ion, which is located about 6 Å away from the zinc ions, is a strong allosteric activator[1] since it stabilizes the active conformation of the enzyme. Replacement of structure-stabilizing Mg^{2+} by other metals alters or even inhibits catalytic activity of native alkaline phosphatases[2] or their mutants.[3]

In synthetic chemistry allosteric tuning of receptor properties by metal ions or organic molecules has been widely explored for supramolecular host–guest systems.[4] Recent examples of positive allostery include Zn^{2+}-induced binding of a fluorescent dye by polyazamacrocycles,[5] and Cs^+-induced binding of C_{60} by a cyclophane host.[6] Negative allostery was demonstrated for diamine binding to a bis-zinc(II) porphyrinic system which is perturbed by Ba^{2+}-coordination to an allosteric crown ether subunit of the host,[7] and for a hydrogen bonding receptor which is deactivated by Cu^I.[8]

Tuning of guest selectivity (naphthalene versus biphenyl) of a hydrophobic host by variation of the allosteric metal (Zn^{2+}, Cu^{2+}) was interpreted as a consequence of different metal coordination geometries which induce different host conformations.[9]

While allostery in host–guest chemistry is well explored, reports on allosteric regulation of synthetic molecular catalysts are rare. Tee and co-workers have observed that the transesterification of nitrophenyl alkanoates by cyclodextrines is accelerated up to 10-fold by addition of alkyl alcohols, carboxylates or sulfonates. Formation of ternary complexes (cyclodextrin–substrate–allosteric effector) was suggested

[a] Prof. Dr. R. Krämer, Dr. I. O. Fritsky,[+] R. Ott, Dr. H. Pritzkow
Anorganisch-Chemisches Institut, Universität Heidelberg
Im Neuenheimer Feld 270, 69120 Heidelberg (Germany)
Fax: (+49) 6221-548439
E-mail: roland.kraemer@urz.uni-heidelberg.de

[+] On leave from Department of Chemistry
Shevchenko University, 01033 Kiev (Ukraine)

  0947-6539/01/0706-1221 $ 17.50+.50/0

on the basis of kinetic data alone.[10] In a similar reaction assay, cleavage of alkyl nitrites by cyclodextrin OH-groups is accelerated by the dodecyltrimethylammonium ion.[11] In both cases, intermolecular reactions are stoichiometric, in fact the cyclodextrin was used in large excess. Rebek has reported an intramolecular cyclization reaction of a functionalized 2,2′-bipyridine which is strongly accelerated by Ni^{II} ions. Complexation of Ni by the bpy chelator imposes preorganization of reactive 6,6′-substituents and facilitates cyclization.[12]

To our knowledge, an abiotic allosteric catalyst which displays turnover behavior has not yet been described. In this paper we report allosteric regulation of a metal-based catalyst for phosphodiester cleavage. In our system two functional metal ions (denoted M_f, Scheme 1) are exposed for direct interaction with the substrate while reactivity is modulated by the identity of a third "structural" metal M_s. Some of these results were recently published as a preliminary communication.[13]

Abstract in German: *Der erste allosterische niedermolekulare Katalysator ist ein dreikerniger Metallkomplex der allgemeinen Formel $(L-H)M_s(M_f)_2$. L steht für einen Polypyridyl-Liganden mit einer vierzähnigen und zwei zweizähnigen Chelateinheiten; M_s ist ein strukturelles (allosterisches) Metallion, und M_f sind funktionelle (katalytische) Metallionen, die direkt mit dem Substrat in Wechselwirkung treten. In den einkernigen $[(L-H)M_s]^+$-Komplexen $[(L-H)Cu(MeOH)]ClO_4$ (**1a**), $[(L-H)Cu]NO_3 \cdot 2H_2O$ (**1b**), $[(L-H)Ni]ClO_4 \cdot 4H_2O$ (**2**) und $[(L-H)Pd]ClO_4 \cdot 2H_2O$ (**3**), dargestellt aus L und M^{2+}-Salzen, wird das Metallion durch N_4-Koordination (für **1a** bestätigt durch eine Kristallstrukturanalyse) stark gebunden. Die Bildung der dreikernigen Komplexe $[(L-H)M_sCu_2]^{5+}$, in denen zwei funktionelle Cu^{2+}-Ionen an die zweizähnigen Bindungsstellen von L koordiniert sind, wurde in Lösung durch photometrische Titrationen und durch die Isolierung von $[(L-H)Cu_3][PO_4][ClO_4]_2 \cdot 9H_2O$ (**4**) nachgewiesen. Die dreikernigen Komplexe katalysieren die Spaltung des RNA-Analogons 2-(Hydroxypropyl)-p-nitrophenylphosphat (HPNP), eines aktivierten Phosphodiesters. Die Gleichgewichtskonstante K_{HPNP} für die Bindung von HPNP an $[(L-H)M_sCu_2]^{5+}$, und die Geschwindigkeitskonstante erster Ordnung k_{cat} für die Spaltung von HPNP, das an den Katalysator gebunden ist, wurden aus der kinetischen Analyse der Spaltungsgeschwindigkeit bei verschiedenen HPNP-Konzentrationen bestimmt: $K_{HPNP} = 170$ $(M_s = Cu^{2+})$, 340 $(M_s = Ni^{2+})$, 2600 $(M_s = Pd^{2+})$ M^{-1}, $k_{cat} = 17 \times 10^{-3}$ $(M_s = Cu^{2+})$, 3.1×10^{-3} $(M_s = Ni^{2+})$, 0.22×10^{-3} $(M_s = Pd^{2+})$ s^{-1}. Offensichtlich wird sowohl die Substrataffinität als auch die Aktivität des Katalysators $[(L-H)M_sCu_2]^{5+}$ durch die Natur des allosterischen Metallions M_s stark beeinflusst. Nach unserer Ansicht ist dies darauf zurückzuführen, dass bereits geringfügige Unterschiede im Ionenradius von M_s und dessen Neigung, die N_4-M_s Koordinationsebene zu verzerren, starken Einfluss auf die Konformation des Katalysators (d.h. die Präorganisation der funktionellen Cu^{2+}-Ionen) und damit auf die katalytische Aktivität haben.*

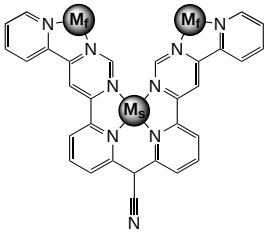

Scheme 1. The allosteric catalyst $[(L-H)M_s(M_f)_2]$, M_s = structural (allosteric) metal, M_f = functional (catalytic) metal.

Results and Discussion

Preparation of the novel polypyridyl ligand L (Scheme 2) which has one tetradentate and two bidentate metal binding sites is outlined only briefly herein, details on synthesis and X-ray structure have been reported elsewhere.[14] L is prepared in two reaction steps starting from 4-(2-pyridyl)-pyrimidine (Scheme 2).[15] Coupling with 2-bromo-6-lithiopyridine[16] gave 4-(6-bromo-2-pyridyl)-6-(2-pyridyl)-pyrimidine. L was obtained analogously to a reported method for 2-quinolyl-2(1*H*)-quinolylideneacetonitrile[17] or related compounds[18] from bromopyridyls and cyanacetamide. It is a dark red solid, the enamine-tautomer was identified by X-ray crystallography.

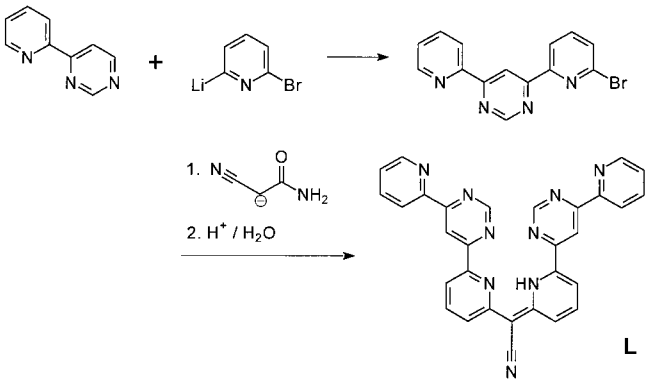

Scheme 2. Synthesis of L.

Mononuclear complexes: L interacts with transitional metal salts in organic solvents in the presence of alkali (KOH), proton substitution occurs immediately for Cu and manifests by color change from wine-red to purple. Formation of Ni and Pd complexes requires elevated temperature. By reaction with M^{2+} salts 1:1 complexes $[(L-H)Cu(MeOH)]ClO_4$ (**1a**), $[(L-H)Cu]NO_3 \cdot 2H_2O$ (**1b**), $[(L-H)Ni]ClO_4 \cdot 4H_2O$ (**2**), and $[(L-H)Pd]ClO_4 \cdot 2H_2O$ (**3**) were obtained in nearly quantitative yields as purple microcrystalline solids and identified as mononuclear complexes by satisfactory elemental analysis, variety of spectroscopic methods and X-ray single crystal analysis of **1a**. Electronic spectra exhibit very intensive bands in the visible and near UV region which are attributed to extended π-conjugation in both L and its complexes. The band in the visible region of L at 499 nm ($\varepsilon = 4040$) undergoes low frequency shift in the spectra of the complexes (524 nm in **1b**,

0947-6539/01/0706-1222 $ 17.50+.50/0 *Chem. Eur. J.* **2001**, *7*, No. 6

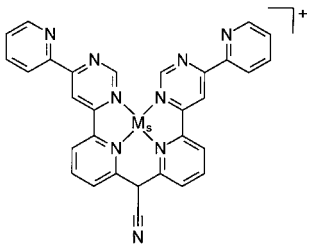

$[(L\text{-}H)M_s]^+$, $M_s = Cu^{II}, Ni^{II}, Pd^{II}$

522 nm in **2**, and 543.5 nm in **3**), accompanied by substantial increase of extinction coefficients ($\varepsilon = 7000$ for **1b**, 7200 for **2**, and 6700 for **3**). It is evident that the diamagnetic Pd complex possesses different spectral properties compared with paramagnetic Ni and Cu (paramagnetism of Ni complex see below). The influence of electronic structure of the metal ion on the UV/Vis spectrum of ligands with extended π-system was discussed for Ni^{II}-porphyrin complexes in which transition from diamagnetic square-planar Ni^{II} to paramagnetic octahedral Ni^{II}, induced by axially coordinating ligands, is accompanied by significant shifts of the optical bands.[19] Formation of $[(L-H)Cu]^+$ from L and Cu^{II} in DMSO/water 1:3 at pH 7 is complete within seconds and could therefore be followed by photometric titration of L with copper(II) nitrate solution. A sharp isobestic point at 463 nm is observed for up to 1 equiv Cu. In contrast, titration with $Ni(NO_3)_2$ and $[Pd(CH_3CN)_4](BF_4)_2$ was complicated by slow formation of the 1:1 complexes at room temperature.

MALDI-MS spectra of solutions of the complexes contain major peaks corresponding only to $[(L-H)M]^+$ patterns with characteristic isotopic distribution for specific metal ions. IR spectra of all isolated complexes indicate, apart of intensive absorption bands corresponding to counterion vibrations (nitrate or perchlorate), sharp peaks attributable to $\tilde{\nu}$(C≡N) stretching mode; these indicate only minor shifts ($\Delta\tilde{\nu} \leq 10\ cm^{-1}$) from its position in the spectrum of the free ligand ($2179\ cm^{-1}$). Absorption in this region is typical for the conjugated nitrile group,[17, 18] so that one can conclude that the coordinated ligand keeps a fully conjugated structure, which is also confirmed by X-ray analysis of **1**. Unlike the spectrum of the free ligand, the spectra of the complexes lack the broad band of $\tilde{\nu}$(pyridyl-N–H) observable at $3448\ cm^{-1}$ in the spectrum of L.

EPR and NMR spectroscopic data of mononuclear complexes are consistent with tetradentate metal coordination. Frozen solutions of copper(II) complexes at concentration of $1 \times 10^{-3} - 5 \times 10^{-4}$ M displayed broad and featureless EPR signals. As in the case of copper(II) porphyrin complexes this is presumably due to aggregation of the molecules during the freezing process.[20] We had to use samples which were diamagnetically diluted with 10-fold excess of L in order to obtain spectra with resolved fine structure. The EPR spectrum of **1** in $CHCl_3$/MeOH glass at 120 K has a superhyperfine structure (nine lines) and is characterized by parameters typical for in-plane N_4-coordination of Cu^{II} ($g_{\|} = 2.207$, $A_{\|} = 196$ G).[21] ^{1}H NMR spectra (solutions in [D$_6$]DMSO) of the diamagnetic square-planar Pd complex and paramagnetic Ni complex contain a single set of resonances and thus suggest C_2 symmetry. For $[(L-H)Ni]^+$ paramagnetic shifts ($\delta = 6.5 - 84$) relative to the spectrum of the free ligand and line broadening is large for five ^{1}H NMR signals belonging to the coordinated py and pym rings. Note, that the signal of the pym-2 proton undergoes the largest downfield shift and was observed at $\delta = 93$ because this proton is closest to the paramagnetic center. Similar paramagnetic shifts were reported for the Ni^{II} complexes with 2,2′-bipyridine.[22] Four signals of $[(L-H)Ni]^+$ which give intensive cross-peaks in ^{1}H,^{1}H-COSY spectrum are shifted less than 2 ppm and thus belong to the uncoordinated py rings. Obviously, in $[(L-H)Ni]^+$ octahedral Ni^{II} with axial solvent coordination is favored in solution rather than a diamagnetic square-planar structure. In the ^{1}H NMR spectrum of the palladium complex only small (< 0.2 ppm) shifts relative to the free ligand are observed, with exception of the pym-2 proton which is shifted downfield by 1.1 ppm. In the NOESY spectrum the signal of pym-5 proton gives an intensive cross-peak with the signal of py-3/py′-3 protons. This indicates that pyrimidine ring is situated in *cis*-position with respect to the internal pyridine ring, as expected for tetradentate coordination of the ligand.

In order to check the stability of complexes **1**, **2**, and **3** with respect to potentially competitive chelating ligands (1,2-diaminoethane, edta), we have treated solutions containing the complexes with an excess of these ligands. 5×10^{-5} M solutions of complexes in DMSO/water 1:3 were treated with 15 equivalents chelating ligand. No evidence of metal abstraction from the complexes was detectable by photometry after 12 h at pH 8.

Crystal and molecular structure of $[(L-H)Cu(MeOH)]ClO_4$ (1a): The molecular structure of **1a** and the numbering scheme is shown in Figure 1, and selected bond lengths, angles and torsion angles are listed in Table 1. Compound **1a** is ionic

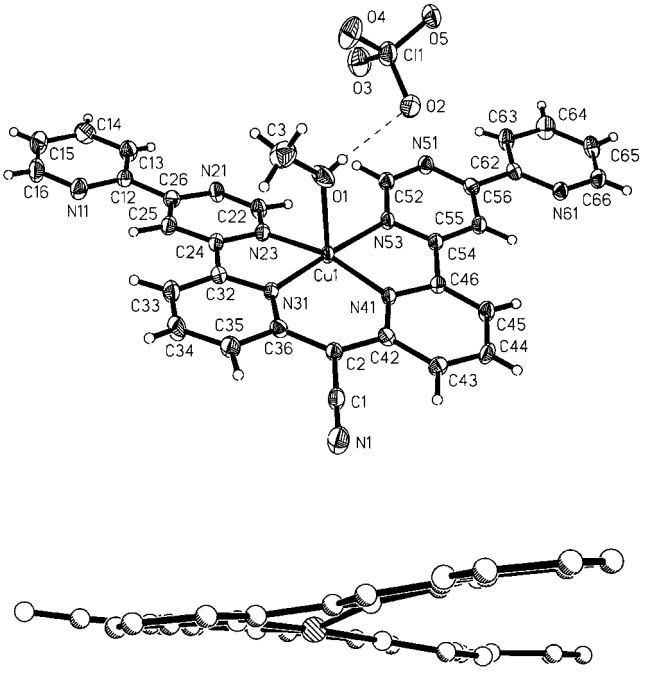

Figure 1. Molecular structure and numbering scheme for **1a** (top). View of the $[(L-H)Cu]^+$ cation (bottom).

Table 1. Selected bond lengths [Å], angles and torsion angles [°] for **1a**.

Cu1–N31	1.978(3)	N31-Cu1-N41	93.17(11)
Cu1–N41	1.978(3)	N31-Cu1-N53	175.06(11)
Cu1–N53	2.037(3)	N41-Cu1-N53	82.20(11)
Cu1–N23	2.047(3)	N31-Cu1-N23	81.74(11)
Cu1–O1	2.253(3)	N41-Cu1-N23	164.76(11)
		N53-Cu1-N23	103.18(11)
		N31-Cu1-O1	90.95(11)
		N41-Cu1-O1	102.98(13)
		N53-Cu1-O1	88.42(11)
		N23-Cu1-O1	91.50(13)
N1–C1	1.147(5)	N1-C1-C2	177.3(5)
C1–C2	1.428(5)	C36-C2-C1	115.4(3)
C2–C36	1.424(4)	C36-C2-C42	128.6(3)
C2–C42	1.433(4)	C1-C2-C42	115.9(3)
N21–C22	1.324(4)	C36-N31-C32	118.8(3)
N23–C22	1.348(4)	N31-C32-C24	114.5(3)
N31–C36	1.362(4)	N31-C32-C33	123.6(3)
N31–C32	1.364(4)	C33-C32-C24	121.8(3)
N41–C42	1.364(4)	C32-C33-C34	117.9(3)
N41–C46	1.365(4)	C35-C34-C33	120.0(3)
N51–C52	1.322(4)	C34-C35-C36	120.4(3)
N53–C52	1.348(4)	N31-C36-C35	119.2(3)
C32–C33	1.367(5)	N31-C36-C2	121.8(3)
C33–C34	1.400(5)	C42-N41-C46	118.6(3)
C34–C35	1.355(5)	N41-C42-C2	122.0(3)
C35–C36	1.426(5)	N41-C42-C43	119.4(3)
C42–C43	1.429(4)	C44-C43-C42	120.4(3)
C43–C44	1.360(5)	C43-C44-C45	119.9(3)
C44–C45	1.399(5)	C46-C45-C44	117.9(3)
C45–C46	1.372(5)	N41-C46-C45	123.7(3)
		C45-C46-C54	121.7(3)
		N41-C46-C54	114.7(3)
C13-C12-C26-C25	175.6(4)		
C25-C24-C32-N31	177.6(3)		
C32-N31-C36-C2	175.1(3)		
C1-C2-C36-N31	–171.7(3)		
C1-C2-C42-N41	178.4(3)		
C42-C2-C36-N31	5.6(6)		
C36-C2-C42-N41	1.1(6)		
C45-C46-C54-N53	179.6(3)		
C55-C56-C62-C63	173.7(4)		

and consists of the complex cation $[(L–H)Cu(MeOH)]^+$ and perchlorate anions, bridged by means of hydrogen bond formed between one of the perchlorate oxygens and methanol (O1 ··· O2 2.795(4) Å). We are not aware of transitional metal complexes of dipyridylacetonitrile or related ligands which have been characterized by X-ray crystallography, and therefore we discuss the structure of **1a** in more detail.

The complex cation of **1a** comprises a distorted square-pyramidal copper(II) ion coordinated in the equatorial plane to four nitrogen atoms of the two internal pyridine and two pyrimidine rings, and to the methanol molecule occupying the apical position. The ligand adopts a helical conformation which is quite close to planar (Figure 1, bottom). It comprises of two nearly planar triaromatic py-pym-py moieties, linked by –C(CN)– spacer. The dihedral angle between these planes is 12.28(9)°. The nitrogen atoms in the terminal py–pym fragments adopt expected *transoid* conformation.

The central dipyridylmethine unit is virtually planar (with maximal deviation from the mean plane observed for C35 by 0.101(3) Å), and the C2–C36 and C2–C42 bond lengths are nearly equal (1.424(3) and 1.433(4) Å, respectively); this indicates delocalization of the negative charge at sp^2-hybridized C2. In the free ligand the corresponding bonds are noticeably different (1.396(3) and 1.454(3) Å) due to non-equivalency between protonated and non-protonated pyridine rings. The value of angle C36-C2-C42 128.6(3)° is close to that in the free ligand (127.3(2)°).

The internal pyridine C–N bond lengths are slightly longer then those typical for pyridine rings (1.362(4) – 1.365(4) Å), which indicates accumulation of negative charge on nitrogen, and there is significant difference in C–C bond lengths: two shorter bonds (1.355(5) – 1.372(5) Å) are alternated with two longer bonds (1.399(5) – 1.426(5) Å) (Table 1). This implies that on substitution of the proton by metal ions the central pyridine rings exist rather in the pyridylidene than in the pyridine form. Similar geometrical features were reported for complexes of the deprotonated bis(pyridyl)methane ligand.[23]

The equatorial N_4 environment co-ordination plane of Cu^{II} displays a slight tetrahedral distortion with nitrogen atoms deviated by 0.103(1) – 0.164(2) Å) alternatively above and below the best plane. The copper atom is raised by 0.115(2) Å toward the apical oxygen O1. The Cu–N(py) distances (Cu1–N31 and Cu1–N41) are equal (1.978(3) Å) and a bit shorter than Cu–N(pym) (Cu1–N53 2.037(3) and Cu1–N23 2.047(3) Å), the axial contact Cu1–O1 2.253(3) Å is much longer, which is typical for copper(II) square-pyramidal complexes. The pyrimidine C22–H ··· H–C52 separation in the complex is only 2.17 Å and corresponds to the van der Waals distance of atoms at a sp^2-carbon (van der Waals H ··· H contact distance for the sp^2 C–H = 2.12 Å, C–H ··· H angle = 120°, 2.22 Å for 130°; the corresponding C–H ··· H angles in **1** are 124 and 125°).[24] Consequently, the helical twist of $[(L–H)Cu]^+$ is important to reduce repulsion of pyrimidine hydrogen atoms. The extent of the helical twist is expected to be very sensitive to the size and stereochemical preferences of the metal ion.

In the case of torsion of two terminal pyridine rings in *cis* position with respect to the adjacent pyrimidine rings, the complex cation has two bidentate bipyridyl-like pockets which are able to coordinate two additional functional metal ions M_f. The N21 ··· N51 separation is 5.568(4) Å, and an M_f ··· M_f distance of about 6 Å is estimated if the M_f–N distance is 2.0 Å.

In the crystal $[(L–H)Cu]^+$ cations form a centrosymmetric dimer (Figure 2) with long axial contact of the copper atom with the C≡N group of the neighboring complex (Cu1 ··· Cu1 $(-x, 1-y, -z)$ 6.278(1) Å, Cu1 ··· N4 $(-x, 1-y, -z)$

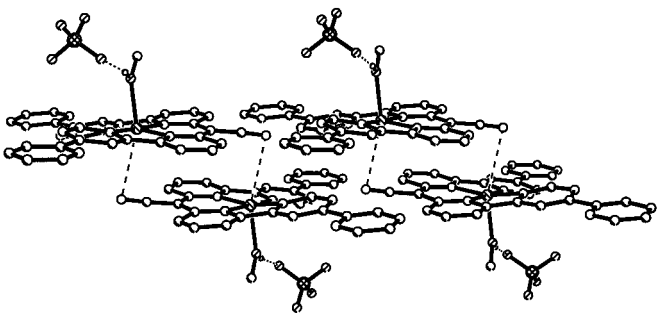

Figure 2. Fragment of the crystal packing of **1a** demonstrating formation of dimers and their organisation into strips.

0947-6539/01/0706-1224 $ 17.50+.50/0 *Chem. Eur. J.* **2001**, *7*, No. 6

3.428(4) Å), and stacking interactions between pairs of symmetrically related internal pyridine rings, with centroid-to-centroid distance of about 3.4 Å. Crystallographic observations support the idea of aggregation of $[(L-H)Cu]^+$ molecules in frozen solutions which gives rise to broadened EPR signals.

Trinuclear complexes: Formation of trinuclear complexes $[(L-H)M_sCu_2]$ in water/DMSO 3:1 solution at pH 7 (which corresponds to the conditions of kinetic experiments on phosphodiester cleavage, see below) was studied by photometric titration of $[(L-H)M_s]^+$ with copper nitrate solution.

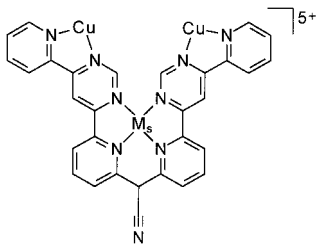

$[(L\text{-}H)M_sCu_2]^{5+}$

2-(hydroxypropyl)-*p*-nitrophenyl phosphate (HPNP) present in reaction solution was replaced by hydrolytically more stable dimethyl phosphate to avoid complication of optical spectra by release of nitrophenyl phosphate ($\lambda_{max} = 400$ nm), the product of intramolecular HPNP cleavage. Batch titrations in the presence of HPNP indicate that—within the limits of experimental error—optical spectra are identical for HPNP- and dimethylphosphate-containing titration solutions. Binding of Cu^{2+} to the bidentate sites of $[(L-H)M_s]^+$ is accompanied by a decrease of absorbance around 520 nm and increase of absorbance around 630 nm, with sharp isosbestic points at 555 nm ($M_s = Cu$, Figure 3), 565 nm ($M_s = Ni$) and

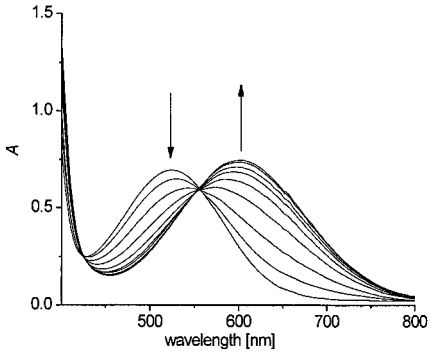

Figure 3. Spectrophotometric titration of $[(L-H)Cu]NO_3$ (10^{-4} M) with copper(II) nitrate in water/DMSO 3:1 solution at pH 7 and 20 °C. Spectra correspond to addition of Cu in 0.5 equiv steps (0 to 4 equiv Cu).

600 nm ($M_s = Pd$). The color of the solutions changes from purple to dark blue in the case of $M_s = Cu$, Ni and to bluish-purple for $M_s = Pd$. The maximum of the optical band of $[(L-H)PdCu_2]^{5+}$ (551 nm) is shifted only 8 nm relative to $[(L-H)Pd]^+$ (543 nm), therefore spectral changes are less significant compared with $[(L-H)Cu_3]^{5+}$ ($\lambda_{max} = 602$ nm) and $[(L-H)NiCu_2]^{5+}$ ($\lambda_{max} = 613$ nm). Absorbance diagrams at 635 nm of the titrations are given in Figure 4a, b.

For $[(L-H)Pd]^+$ the absorbance increases almost linearly for 0 to 2 equiv Cu and levels off at >2 equiv Cu (absorbance of free Cu^{2+} is negligible). In contrast, excess Cu is required

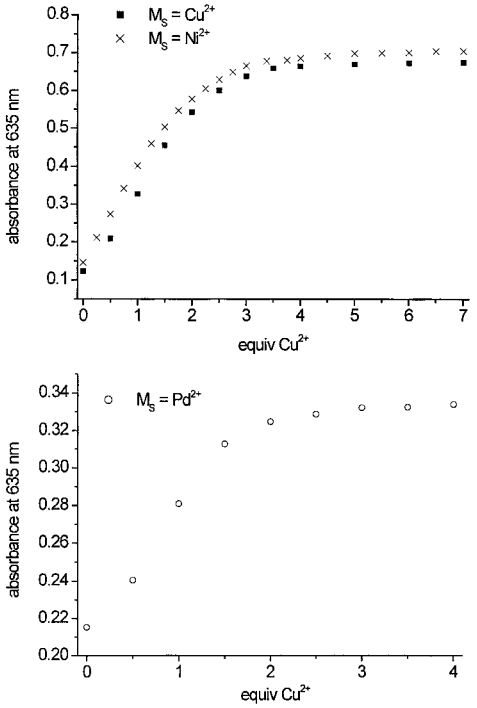

Figure 4. Increase of 635 nm absorbance on photometric titration of $[(L-H)M_s]^+$ (10^{-4} M) with copper nitrate solution. Water/DMSO 3:1, pH 7.0, 5×10^{-4} M Na-dimethyl phosphate, buffer 5 mM 3-(N-morpholino)-propanesulfonic acid (MOPS), $T = 20$ °C, a) $M_s = Cu$, Ni, b) $M_s = Pd$.

for nearly quantitative formation of complexes $[(L-H)Cu_3]^{5+}$ and $[(L-H)NiCu_2]^{5+}$, indicating a lower affinity of Cu^{2+} to $[(L-H)Cu]^+$ and $[(L-H)Ni]^+$.

Trinuclear complexes are substantially stabilized by addition of phosphate which is expected to bridge the two functional Cu ions and overcome electrostatic repulsion between the metal cations. When the titrations of Figure 4a are performed in the presence of KH_2PO_4 (1 equiv), nearly quantitative formation of $[(L-H)Cu_3]^{5+}$ and $[(L-H)NiCu_2]^{5+}$ on addition of 2.0 equiv Cu^{2+} is indicated by the absorbance profiles (no significant increase of absorbance at >2 equiv Cu). The titration profile of $[(L-H)Pd]^+$ (Figure 4b) is not affected by KH_2PO_4 since the trinuclear complex is formed quantitatively even in the absence of phosphate.

When the pH is lowered from 7 to 5 by addition of HNO_3 in unbuffered titration solutions, a shift in the equilibrium toward the mononuclear complex $[(L-H)M_s]^+$ is detectable. Since we have no evidence for significant protonation of pyridyl groups at pH 5, this effect may be related to the protonation of Cu-coordinated hydroxide present at pH 7 (pK_a of (bpy)Cu-coordinated water is 7.9 at 25 °C).[25] Thus, Cu-coordinated hydroxide may reduce electrostatic repulsion of Cu^{2+} ions in $[(L-H)M_sCu_2]^{5+}$.

Binding of two Cu^{2+} ions to $[(L-H)M_s]^+$ may proceed with positive, negative, or without any cooperativity at all. While

the spectra of complexes $[(L-H)M_sCu_2]^{5+}$ are obtained by titration with excess Cu^{2+}, the spectra of dinuclear complexes $[(L-H)M_sCu]^{3+}$ are not available. The optical spectrum of the isolated dinuclear complex $[(L-H)Cu_2]Cl_3$ (see below) in DMSO/MeOH 1:1 solution is similar to the sum of the spectra of $[(L-H)Cu]^+$ and $[(L-H)Cu_3]^{5+}$. Therefore, it appears to be difficult to distinguish even the extreme cases between the positive cooperativity with exclusive formation of $[(L-H)M_sCu_2]^{5+}$, and the negative cooperativity with exclusive formation of $[(L-H)M_sCu]^{3+}$ at 1 equiv Cu^{2+}. Therefore we cannot draw any conclusions from photometric titrtrations on cooperative incorporation of Cu by $[(L-H)M_s]^+$ (although kinetic data (Figure 5) rather suggest a positive cooperativity, assuming that the dinuclear complexes are much less reactive than the trinuclear complexes).

To make sure that Cu does not substitute Ni and Pd in the tetradentate site under the conditions of kinetic experiment in the $[(L-H)NiCu_2]^{5+}$ and $[(L-H)PdCu_2]^{5+}$ complexes, we have investigated solutions containing $[(L-H)M_s]^+$ and 4 equiv Cu^{2+} (conditions see legend of Figure 5), kept at 20 °C for three days, by MALDI mass spectrometry. Under ionization conditions labile metals at bidentate sites dissociate off and an intensive $[(L-H)M_s]^+$ peak is observed. Since we found only $[(L-H)Ni]^+$ and $[(L-H)Pd]^+$ patterns as major peaks and only traces (<1%) of $[(L-H)Cu]^+$, metal exchange at the tetradentate site is insignificant. (In control experiments, mixtures of freshly prepared $[(L-H)M_s]^+$ (M_s = Ni, Pd)+4 Cu and $[(L-H)Cu]^+$+4 Cu gave patterns of $[(L-H)M_s]^+$ and $[(L-H)Cu]^+$ in the expected ratio). In more rigid conditions (solutions were kept at 50 °C during 4 h), in case of the Ni complex substitution at the tetradentate site occurs to a small extent: The relative ratio of Ni and Cu isotopic patterns is about 9:1. In the case of the Pd complex, only minor signals corresponding to Cu pattern were observed (<1% the intensity of the Pd pattern). In kinetic studies (see below) initial rates were detected for reaction times <15 min at 20 °C. Therefore, significant exchange of tetradentate Ni or Pd by Cu in $[(L-H)M_sCu_2]^{5+}$ is negligible.

We have attempted to prepare trinuclear complexes $[(L-H)Cu_3]$ by addition of two equivalents of copper(II) nitrate or acetate to a solution of $[(L-H)Cu](NO_3)$ complex in methanol (addition is accompanied by color change from purple to blue). Dark blue powders were obtained by precipitation with saturated aqueous sodium perchlorate. The products obtained, however, failed to give satisfactory analytical data. According to ball-and-stick models the tetrahedral PO_4^{3-} anion satisfies geometric requirements for a triatomic angular bridging coordination to $[(L-H)Cu_3]$. Also, highly charged phosphate anion is a good donor and efficiently compensates electrostatic repulsion of Cu^{2+} in the trinuclear complex. In this juncture, the aforementioned stabilizing role of phosphate anion in formation of trinuclear complexes becomes understandable. Moreover, addition of one equivalent phosphate results in complete inhibition of phosphodiesterase activity of trinuclear complexes in solution discussed below. By reaction of $[(L-H)Cu]^+$ with two equivalents copper perchlorate and Na_3PO_4, followed by precipitation with aqueous $NaClO_4$, we have obtained a dark-blue microcrystalline complex which gave correct elemental analysis for $[(L-H)Cu_3][PO_4][ClO_4]_2 \cdot 9H_2O$ (**4**).

The electronic spectrum of **4** (absorption maximum at 587 nm, $\varepsilon = 7000$, DMSO) reminiscent of that obtained in the titration of $[(L-H)Cu]^+$ in the presence of one equivalent KH_2PO_4 at two (or more) equivalents Cu (maximum at 602 nm, $\varepsilon = 7600$, water/DMSO 3:1). The EPR spectrum at 110 K (in DMSO/MeOH 1:1) exhibits a broad asymmetric feature at $g = 2.08$ with no resolved fine structure and no signal at half-field.

Reaction of L with one equivalent copper(II) chloride and one equivalent base followed by addition two more equivalents copper(II) chloride resulted in formation of blue-violet precipitate for which we suggest a dinuclear structure $[(L-H)Cu_2]Cl_3 \cdot 3H_2O$ (**5**) based on microanalysis. It means that chloride ions are not capable to support trinuclear coordination, according to ball and stick models Cl^- cannot bridge two copper atoms coordinated at bidentate sites. Rather, a trinuclear complex is destabilized by mutual steric repulsion of two Cu-coordinated Cl^- ions. Complex **5** has an absorption maximum at 535 nm ($\varepsilon = 9000$, DMSO/MeOH 1:1), and broad featureless signal in the EPR spectrum with $g = 2.07$ both at 115 and 300 K (DMSO/MeOH 1:1).

Catalytic phosphodiester cleavage: We have examined the reactivity of $[(L-H)M_sCu_2]^{5+}$ toward nitrophenyl phosphate mono- and diesters. Only minor activity was detected with bis(*p*-nitrophenyl)phosphate and (*p*-nitrophenyl)phosphate while the complex with M_s = Cu in particular is highly reactive toward the RNA analogue HPNP. HPNP is widely used to investigate phosphoesterase activity of metal complexes. Intramolecular cyclization of this phosphodiester (Scheme 3) is easily followed photometrically by the 400 nm

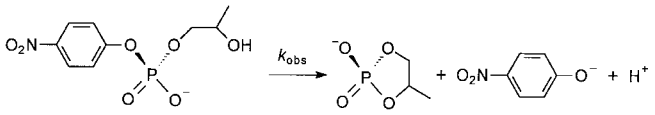

HPNP

Scheme 3. Intramolecular cleavage of the phosphodiester 2-(hydroxypropyl)-*p*-nitrophenyl phosphate (HPNP).

absorbance of released nitrophenolate. First, kinetic studies at varying Cu^{2+} concentrations were performed in a buffered water/DMSO 3:1 mixture at pH 7.0, 10^{-4} M complex concentration and 5×10^{-4} M HPNP. With mononuclear complexes $[(L-H)M_s]^+$ (at $[Cu^{2+}] = 0$, Figure 5) HPNP cleavage rate is very low ($k_{obs} < 2 \times 10^{-6}\ s^{-1}$) since the Pd complex is saturated coordinatively and interaction with the substrate at a single axial coordination site (for Ni and eventually Cu complexes) provides at best modest activation.

Cleavage rate increases dramatically when Cu^{2+} is added to $[(L-H)M_s]^+$ (Figure 5). In reasonable agreement with photometric results (Figure 4) >2 equiv Cu are required for quantitative formation of $[(L-H)M_sCu_2]^{5+}$ and maximum level of activity, although no further increase of rate at >2.5 equiv Cu and even some decrease at >4 equiv Cu is observed.[26] Many examples for the efficient cleavage of

0947-6539/01/0706-1226 $ 17.50+.50/0 *Chem. Eur. J.* **2001**, *7*, No. 6

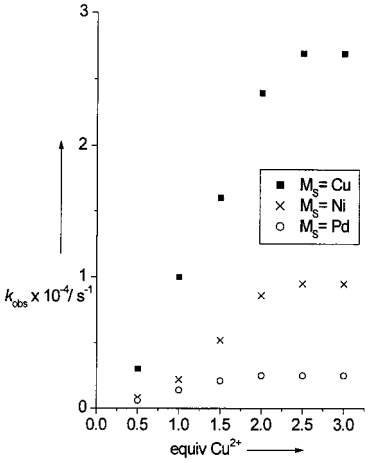

Figure 5. k_{obs} for cleavage of HPNP (5×10^{-4} M) by $[(L{-}H)M_s]^+$ (10^{-4} M) at varying copper(II) nitrate concentrations. Water/DMSO 3:1, pH 7.0, buffer 5 mM MOPS, $T = 20\,^{\circ}C$. Catalysis by free Cu^{2+} ($k_{obs} = 2.5 \times 10^{-6}\,s^{-1}$ at 10^{-4} M Cu^{2+}) was neglected. Average values of three kinetic runs, reproducible within 15%.

phosphate esters by cooperation of two metal ions in phosphoesterase model complexes have been reported.[27] In its reactivity toward HPNP our system with two functional Cu ions is comparable to other dicopper(II) artificial phosphoesterases.[28]

Kinetics of HPNP cleavage was explored in more detail using complexes prepared in situ from $[(L{-}H)Cu](NO_3)$ and three equivalents copper(II) nitrate. On the basis of photometric data (Figure 4) we estimate that >85% of $[(L{-}H)Cu]^+$ is converted to the trinuclear complex under these conditions. Kinetic parameters were derived from initial rates only because the analysis is complicated for prolonged reaction times by competitive binding of product (cyclic phosphodiester) to the catalyst. The reaction is first order in complex concentration (range $0.5-3 \times 10^{-4}$ M), and first order in HPNP at low concentration ($10^{-4}-10^{-3}$ M). With 2.5 mM HPNP and 10^{-4} M complex at least two catalytic turnovers without loss of activity were detected. Addition of one equivalent PO_4^{3-} per complex completely inhibits cleavage of HPNP while addition of 5 equiv $NaClO_4$ or $NaNO_3$ has no effect on k_{obs}.

Remarkably, the reactivity of complexes $[(L{-}H)M_sCu_2]^{5+}$ toward HPNP strongly depends on the structural metal M_s. $[(L{-}H)NiCu_2]^{5+}$ is three times and $[(L{-}H)Cu_3]^{5+}$ is even ten times more reactive than $[(L{-}H)PdCu_2]^{5+}$.

pH Rate profiles (Figure 6) are very similar for the three complexes, with a maximum at pH 6.5–7, a slight decrease of activity (by about 20%) when pH is lowered to 6 and a significant decrease of activity (by 30–60%) at pH 7.5 At higher pH copper hydroxide precipitate forms, and at pH ≤ 5 the trinuclear complex dissociates to some extent into $[(L{-}H)M_s]^+$ and free Cu^{2+} ions. A bell shaped pH rate profile is often observed for metal-promoted HPNP cleavage. The increase of rate with increasing pH is explained by generation of metal-promoted hydroxide which acts as a general base in HPNP cleavage (alternatively free hydroxide might deprotonate the alcohol group of the substrate). The decrease of rate at higher pH might reflect competitive binding of hydroxide to the catalyst which prevents binding of the substrate. Although this is not clear in detail which factors contribute to the shape of the pH rate profiles in Figure 6, it seems unlikely that Cu-coordinated water has very different pK_a values for different M_s. This would give rise to different maxima in the profiles.

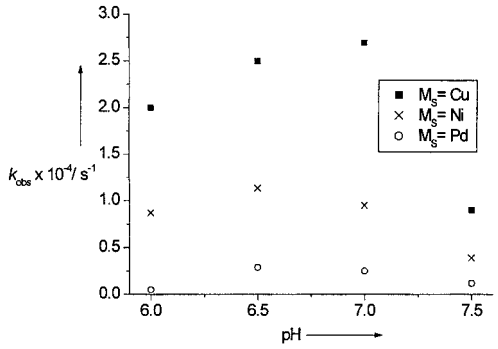

Figure 6. Dependence of k_{obs} on pH for cleavage of HPNP (5×10^{-4} M) by $[(L{-}H)M_sCu_2]^{5+}$ ($\approx 10^{-4}$ M, prepared in situ from **1b**, **2**, or **3** (10^{-4} M) and excess copper(II) nitrate (3×10^{-4} M)). Water/DMSO 3:1, pH 6.0, 6.5: 5 mM 2-(n-morpholino)ethanesulfonic acid (MES) buffer; pH 7.0, 7.5: 5 mM MOPS buffer, $T = 20\,^{\circ}C$. Average values of three kinetic runs, reproducible within 15%.

Saturation behavior in catalytic HPNP cleavage was explored at varying substrate concentrations and 10^{-4} M complex concentration. Again, trinuclear complexes were prepared from $[(L{-}H)M_s]^+$ (10^{-4} M) and 3 equiv Cu^{2+}, with some uncertainty about the exact concentration of the trinuclear complex ($> 0.85 \times 10^{-4}$ M). A Lineweaver–Burke plot (Figure 6) illustrates the linear dependence of reciprocal initial rate $(dc/dt)^{-1}$ on reciprocal substrate concentration. Thus, catalysis follows in good approximation Michaelis–Menten law for a HPNP concentration range 1.5×10^{-4} to 2.5×10^{-3} M (in case of Pd data at HPNP concentrations <0.3 mM are not included since cleavage was too slow to be measured accurately).

From the plots in Figure 7 the values of k_{cat} (first order rate constant for the cleavage of HPNP when bound to the

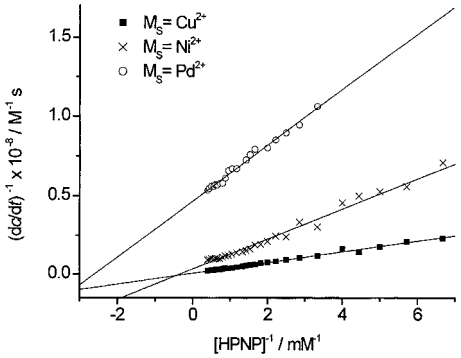

Figure 7. Lineweaver–Burke plot for catalytic HPNP cleavage dependence of $(dc/dt)^{-1}$ on $[HPNP]^{-1}$. Catalysts $[(L{-}H)M_sCu_2]^{5+}$ were prepared in situ from **1b**, **2**, or **3** (10^{-4} M) and excess copper(II) nitrate (3 equiv, 3×10^{-4} M). Water/DMSO 3:1, pH 7.0, 5 mM MOPS buffer, $T = 20\,^{\circ}C$. Catalysis by free Cu^{2+} ($k_{obs} = 2.5 \times 10^{-6}\,s^{-1}$ at 10^{-4} M Cu^{2+}) was neglected. Average values of three kinetic runs, reproducible within 20%.

catalyst) and of K_M (Michaelis constant) were derived, using the following equation:

$$(dc/dt)^{-1} = (k_{cat} \cdot [catalyst])^{-1} + (K_M \cdot k_{cat} \cdot [catalyst] \cdot [HPNP]_0)^{-1}$$

and implying that concentration of the trinuclear catalyst is 10^{-4} M. $K_{HPNP} = (K_M)^{-1}$ corresponds to the equilibrium constant for binding of HPNP to $[(L-H)M_sCu_2]^{5+}$. The difference in k_{cat} values is very significant (Table 2): $[(L-H)Cu_3]^{5+}$ cleaves HPNP six times faster than $[(L-H)NiCu_2]^{5+}$ and 77 times faster than $[(L-H)PdCu_2]^{5+}$. A reverse trend is found for K_{HPNP}, substrate affinity of $[(L-H)PdCu_2]^{5+}$ is eight times higher than of $[(L-H)NiCu_2]^{5+}$ and 16 times higher than for $[(L-H)Cu_3]^{5+}$. Previously determined HPNP binding constants of dinuclear copper(II) and zinc(II) complexes in water range from 10^2 to 5×10^4 M^{-1} and depend on preorganization of the metal ions and on competition with metal bound hydroxide.[27c, 29] Cyclization of $[(L-H)Cu_3]^{5+}$-bound HPNP at 25 °C is about 10^6 times faster than the uncatalysed reaction at pH 7 and 25 °C, for which we have measured $k_{obs} = 1.2 \times 10^{-8}$ s^{-1} in water/DMSO 3:1 medium at 40 mM HPNP concentration, and about 10^2 times faster than the Cu^{2+}-ion mediated reaction (literature: $k_{cat} = 6 \times 10^{-4}$ s^{-1} at 37 °C and pH 6.85 in water);[30] for $[Cu^{2+}] = 10^{-4}$ M and $[HPNP] = 5 \times 10^{-4}$ M we have measured $k_{obs} = 2.5 \times 10^{-6}$ s^{-1}, compared with 2.7×10^{-4} s^{-1} for $[(L-H)Cu_3]^{5+}$, conditions see Figure 5. It is obvious that the structural metal M_s in complexes $[(L-H)M_sCu_2]^{5+}$ has substantial influence on both substrate affinity and catalytic efficiency.

Table 2. Catalytic cleavage of HPNP by catalyst $[(L-H)M_sCu_2]^{5+}$, values of K_{HPNP} (formation constant of catalyst–HPNP complex) and k_{cat} (rate constant for the cleavage of catalyst-bound HPNP), derived from Lineweaver-Burke plot, see Figure 6.

M_s	K_{HPNP} [M^{-1}]	k_{cat} [s^{-1}]
Cu^{2+}	170	17×10^{-3}
Ni^{2+}	340	3.1×10^{-3}
Pd^{2+}	2600	0.22×10^{-3}

In our view this must be a consequence of different catalyst conformations aligned with varying preorganization of the functional copper ions. Even subtle differences in the ionic radius of M_s and its tendency to distort the N_4-M_s plane of coordination are expected to have substantial influence on the helical twist of the ligand framework (compare Figure 1) and consequently on M_f-M_f distance and relative orientation of M_f coordination polyhedra.

Copper(II)-mediated catalysis of HPNP cleavage is usually attributed to Lewis acid activation of the substrate and action of Cu-OH as a general base which promotes intramolecular nucleophilic attack of the alcohol group.[30] These features should also be relevant in the catalysis by $[(L-H)M_sCu_2]^{5+}$, but mechanistic details cannot be derived from kinetic data.

Remarkably, the catalytically most active complex $[(L-H)Cu_3]^{5+}$ has the lowest affinity for HPNP. Additionally, functional Cu^{2+} is bound more labile compared with $[(L-H)PdCu_2]^{5+}$. This can be interpreted in terms of a destabilized ground state (i.e., the HPNP-catalyst complex), reflected by low binding constants of both HPNP and functional Cu^{2+}. Ground state destabilization contributes to rate acceleration by reducing the energy gap between ground state and transition state and is recognized as an important motif of enzymatic catalysis. Apparently, in $[(L-H)Cu_3]^{5+}$ the structural copper ion induces a change in the conformation which disfavors (compared with complexes having M_s = Ni, Pd) HPNP binding so that the catalyst–substrate complex is relatively high in energy. On the other hand, the trigonal-bipyramidal transition state of the intramolecular nucleophilic substitution at phosphorus must be substantially stabilized.

We have considered other effects which may contribute to the different reactivities of complexes $[(L-H)M_sCu_2]^{5+}$. A potential role of axial coordination sites at M_s (M_s = Cu, Ni) in substrate activation was examined with ball-and-stick models. A direct interaction of the M_f-coordinated phosphodiester with M_s, that is bridging of M_f and M_s by the phosphate group, appears sterically impossible. Even hydrogen bonding of axial M_s-H_2O with M_f-coordinated phosphate ester is disfavored. Also, efficient cooperation of two copper ions across the bridging pyrimidine moiety is ruled out experimentally. The in situ prepared dinuclear copper(II) complex of 4,6-di(2-pyridyl)pyrimidine $[(py_2pym)Cu_2]^{4+}$ cleaves HPNP with a first order rate constant of only 8×10^{-6} s^{-1} under the conditions of Figure 5.

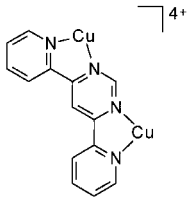

$[(py_2pym)Cu_2]^{4+}$

A potential influence of M_s on the Lewis acidity of functional Cu^{2+} ions is another effect which is worth considering. In 1:1 copper(II) complexes with bidentate *N,N*-chelators the π-acceptor properties of the ligand influence the stability of ternary complexes with oxoanions and reactions of the latter in which Cu^{2+} acts as a Lewis acidic activator.[31] However, even dramatic variation of the π-acceptor capacity of the ligand has only moderate effect on reaction rate, for example when 2,2′-bipyridine is replaced by aliphatic amines rate decreases about two-fold.[31] Even if different M_s^{2+} ions impose subtle differences in charge distribution of the extended π-system of the ligand, we do not believe that this significantly influences Lewis acidity of Cu.

Conclusion

In conclusion, our system may be considered as a prototype of a synthetic allosteric catalyst having well defined catalytic and allosteric subunits. In the typical case of enzyme regulation by metals the latter reversibly bind to the allosteric site as external modifiers. We cannot investigate the reactivity of $[(L-H)M_sCu_2]^{5+}$ in the absence of the allosteric metal. We see, however, certain parallels to alkaline phosphatases in which replacement of a structural Mg^{2+} by other divalent metals strongly influences the catalytic activity mediated by two

0947-6539/01/0706-1228 $ 17.50+.50/0 *Chem. Eur. J.* **2001**, *7*, No. 6

functional Mg^{2+} ions. Another remarkable aspect is the straightforward possibility of fine-tuning preorganization of the two functional metal ions M_f by variation of the structural metal M_s. This will allow the systematic investigation of metal–metal cooperativity in various reactions for a range of M_f–M_f distances and relative orientation of M_f coordination polyhedra. Other approaches to this problem have been described but require elaborate synthesis of a set of binucleating ligands with different spacing groups.[32]

Experimental Section

General procedures and methods: Syntheses were carried out under nitrogen in dry solvents using standard Schlenk technique, while work up was performed using grade solvents on the air. Ligand L was synthesized according to the procedure reported previously.[14] 2-(Hydroxypropyl)-*p*-nitrophenyl phosphate (HPNP) was prepared as its barium(II) salt, following a reported procedure.[33] The metal salts were reagent grade and used without further purification. ^{1}H and ^{13}C NMR spectra were obtained on Bruker AC-300 (300.13 MHz) and Bruker AC-400 (400.13 MHz) spectrometers, chemical shifts are reported in ppm downfield from Me_4Si. Assignment of the signals in ^{1}H and ^{13}C NMR spectra was obtained with ^{1}H,^{1}H and ^{1}H,^{13}C COSY spectra. IR spectra were recorded on a Perkin–Elmer 983 G spectrometer. Field desorption (FD) and matrix-assisted laser desorption/ionization (MALDI) (2-(4-hydroxyphenylazo)-benzoic acid matrix) mass spectra were recorded with a Finnigan MAT 8230 instrument. Absorbance UV/Vis spectra of solutions were registered on a Specord S100 spectrophotometer (Carl Zeiss Jena). The EPR spectra of solid samples and frozen solutions were recorded on a Bruker ESP 300E spectrometer at X band (9.3 GHz) at 120 and 300 K. For spectrophotometric and kinetic measurements deionised water and reagent grade solvents (DMSO, methanol) were used, the solutions were handled in the air. Elemental analyses were performed by the Microanalytisches Laboratorium des Organisch-Chemischen Instituts der Universität Heidelberg.

Spectrophotometric titrations (Figure 4): Solutions of the mononuclear complexes **1a**, **2**, or **3** (0.1 mM), (3-[*N*-morpholino]propanesulfonic acid)-buffer (MOPS) (0.05 M, pH 7.0) and sodium dimethylphosphate (0.5 mM) were prepared in water/DMSO 3:1. Appropriate amounts of a $Cu(NO_3)_2 \cdot 3H_2O$ stock solution (2 mM in water/DMSO 3:1) were added. About 30 s after addition of metal salt UV spectra were recorded at 25 °C. On prolonged standing of the solutions no further spectral changes with time were detectable.

Kinetic studies: Reaction solutions were prepared by combining appropriate amounts of the mononuclear complexes **1b**, **2**, or **3** (0.4 mM stock solutions in DMSO), $Cu(NO_3)_2 \cdot 3H_2O$ (2 mM stock solution in H_2O), and MOPS buffer (0.5 M stock solution in H_2O, pH 7.0). The reaction was started by addition of the substrate HPNP (5 mM stock solution in H_2O). For the experiments are summarised in Figure 5, final concentrations in the reaction mixtures were 0.1 mM complex, 0.5 mM HPNP and 0.05 M MOPS buffer in water/DMSO 3:1, the concentration of $Cu(NO_3)_2$ varied from 0 to 0.3 mM. Transesterification of HPNP was followed spectrophotometrically by the release of *p*-nitrophenolate at 400 nm ($\varepsilon = 18\,600\ M^{-1}cm^{-1}$), considering equilibration *p*-nitrophenol/*p*-nitrophenolate at pH 7.0 (pK_a 7.15). The pseudo first order rate constants k_{obs} were determined from the initial rate of the reaction (< 5% conversion). All reported data are average values of at least three measurements (reproducibility < 15%).

Determination of k_{cat} and K_M by UV/Vis measurements was performed in microplates on a Tecan Spectrafluor Plus spectrophotometer, reaction solutions were prepared by a robotic liquid handling system (Genesis 150 workstation, Tecan). MOPS buffer (0.5 M stock solution in H_2O, pH 7.0), water, and HPNP (varying concentrations from 0.1 mM to 10 mM in H_2O) were added to solutions of the mononuclear complexes **1b**, **2**, or **3** (0.4 mM stock solution in DMSO). Final concentrations in the reaction mixtures were 0.1 mM complex and 0.05 mM MOPS buffer in water/DMSO 3:1, HPNP concentrations varied from 0.025 to 2.5 mM. Reactions were started by addition of 2.5 equiv $Cu(NO_3)_2 \cdot 3H_2O$ (1.2 mM stock solution in H_2O). Transesterification of HPNP was followed spectrophotometrically by the release of *p*-nitrophenolate at 430 nm ($\varepsilon = 13\,000\ M^{-1}cm^{-1}$), considering equilibration *p*-nitrophenol/*p*-nitrophenolate at pH 7.0 (pK_a 7.15). The pseudo first order rate constants k_{obs} were determined from the initial rate of the reaction (< 5% conversion). All reported data are average values of three measurements (reproducibility < 20%).

Caution! Transition metal perchlorate complexes are potentially explosive and should be handled with utmost care and in small quantities!

Ligand L (for comparison with complexes selected spectroscopic data are given): MS (FD): *m/z* (%): 505.5 (100) $[M]^+$; ^{1}H NMR (300.13 MHz, [D$_6$]DMSO): $\delta = 7.57$ (ddd, 2H, $J_{3,5} = 1.1$, $J_{4,5} = 7.7$, $J_{5,6} = 4.8$ Hz, py-5,), 7.84 (d, 2H, $J_{4,5} = 7.8$ Hz, py′-5), 8.01 (td, 2H, $J_{3,4} = 7.7$, $J_{4,6} = 1.2$ Hz, py-4), 8.11 (t, 2H, $J_{3,4} = 7.8$ Hz, py′-4), 8.29 (m, 2H, py-3), 8.40 (d, 2H, py′-3), 8.73 (d, 2H, py-6), 8.75 (d, 2H, $J_{2,5} = 1.1$ Hz, pym-2), 9.24 (d, 2H, pym-5), 16.02 (s, 1H, NH); ^{13}C NMR ($CDCl_3$, 75.47 MHz): $\delta = 70.88$ [C(C≡N)], 113.28 (py′-5), 113.59 (pym-5), 121.65 (py-3), 122.04 (C≡N), 122.71 (py′-3), 125.27 (py-5), 137.89 (py′-4), 137.00 (py-4), 146.72 (py′-6), 149.14 (py-6), 152.91 (py-2/2′), 155.13 (py-2/2′), 158.37 (pym-2), 160.64 (pym-4/6), 163.04 (pym-4/6); UV/Vis (DMSO): λ_{max} (ε) = 382 (14 600), 499 nm (4040 $mol^{-1}dm^3cm^{-1}$); IR (KBr): $\tilde{\nu} = 2179$ (C≡N), 3448 br (N–H) cm^{-1}; elemental analysis calcd (%) for $C_{30}H_{19}N_9$ (505.5): C 71.28, H 3.79, N 24.94; found: C 71.15, H 3.92, N 24.66.

[(L–H)M$_s$X]*n*Solv (X = NO_3^-, ClO_4^-; Solv = MeOH or H_2O). Ligand L (20 mg, 0.04 mmol) was dissolved in CH_2Cl_2 (10 mL), then methanol (20 mL) and aq KOH (1 M, 0.04 mL) were added. To this reaction mixture the aqueous solution of the corresponding metal salt (copper(II) or nickel(II) nitrate (1 M, 0.04 mL) or $[Pd(CH_3CN)_4](BF_4)_2$ (17.5 mg, 0.04 mmol, dissolved in 5 mL acetonitrile) was added on stirring. The reaction mixture was stirred and heated at 40–60 °C for 30 min. After cooling excess 1 M aqueous solution of potassium nitrate or sodium perchlorate, respectively, was added (10 mL). The precipitates were filtered, washed with water, and dissolved on a filter in warm methanol or, in the case of palladium complex, in hot methanol/acetonitrile 1:1 mixture. Complexes were precipitated by addition of diisopropyl ether, separated by centrifugation, washed with diethyl ether, and dried in vacuo.

[(L–H)Cu(MeOH)]ClO_4 (1a): Dark red-violet needle-shaped crystals (19 mg, 68%) suitable for X-ray analysis were grown by slow diffusion of diethyl ether vapors into saturated solution of **1a** in methanol. MALDI-MS: *m/z* (%): 567.0 (100) $[^{63}Cu(L–H)]^+$), 569.0 (54) $[^{65}Cu(L–H)]^+$; IR (KBr pellets): $\tilde{\nu} = 2172$ (C≡N), 1108 (Cl–O), 624 (δ(Cl–O)) cm^{-1}; elemental analysis calcd (%) for $CuC_{31}H_{22}N_9ClO_5$ (699.6): C 53.22, H 3.17, N 18.02; found: C 53.29, H 3.34, N 17.88.

[(L–H)Cu]$NO_3 \cdot 2H_2O$ (1b): Yield: 17 mg, 64%; MALDI-MS: *m/z* (%): 567.0 (100) $[^{63}Cu(L–H)]^+$, 569.0 (54) $[^{65}Cu(L–H)]^+$; UV/Vis (H_2O/DMSO 3:1): λ_{max} (ε) = 384 (16 000), 524 nm (7000 $mol^{-1}dm^3cm^{-1}$); IR (KBr): $\tilde{\nu}$ = 2178 (C≡N), 1358 (N–O nitrate) cm^{-1}; elemental analysis calcd (%) for $CuC_{30}H_{22}N_{10}O_5$ (666.1): C 54.09, H 3.33, N 21.03; found: C 54.24, H 3.13, N 20.93.

[(L–H)Ni]$ClO_4 \cdot 4H_2O$ (2): Yield: 21 mg, 71%; MALDI-MS: *m/z* (%): 562.0 (100) $[^{58}Ni(L–H)]^+$, 564.0 (39) $[^{60}Ni(L–H)]^+$; ^{1}H NMR (300.13 MHz, [D$_6$]DMSO): $\delta = 7.99$ (s, 2H, py-5), 9.04 (s, 2H, py-4), 9.47 (s, 2H, py-3), 10.80 (s, 2H, py-6), 14.58 (s, 2H, pym-5 or py′-4), 45.82 (br s, 2H, pym-5 or py′-4), 61.62 (br s, 2H, py′-3 or py′-5), 63.25 (br s, 2H, py′-3 or py′-5), 93.08 (br s, 2H, pym-2); UV/Vis (H_2O/DMSO 3:1): λ_{max} (ε) = 384 (25 600), 522 nm (7200 mol^{-1} dm^3 cm^{-1}); IR (KBr): $\tilde{\nu} = 2171$ (C≡N), 1099 (Cl–O), 625 (δ(Cl–O)) cm^{-1}; elemental analysis calcd (%) for $NiC_{30}H_{26}N_9ClO_8$ (734.7): C 49.04, H 3.57, N 17.16; found: C 48.88, H 3.61, N 16.87.

[(L–H)Pd]$ClO_4 \cdot 2H_2O$ (3): Yield: 24 mg, 80%; MALDI-MS: *m/z* (%): 607.9 (27) $[^{104}Pd(L–H)]^+$, 608.9 (72) $[^{105}Pd(L–H)]^+$, 609.9 (100) $[^{106}Pd(L–H)]^+$), 611.9 (74) $[^{108}Pd(L–H)]^+$, 613.9 (37) $[^{110}Pd(L–H)]^+$; ^{1}H NMR (300.13 MHz, [D$_6$]DMSO): $\delta = 7.69$ (ddd, 2H, $J_{4,5} = 7.7$, $J_{5,6}$ = 4.2 Hz, py-5), 7.82 (d, 2H, $J_{4,5} = 7.7$ Hz, py′-5), 7.95 (t, 2H, $J_{3,4} = 7.7$ Hz, py′-4), 8.08 (td, 2H, $J_{3,4} = 7.7$, $J_{4,6} = 1.2$ Hz, py-4), 8.42 (d, 4H, py-3+py′-3), 8.78 (d, 2H, py-6), 9.13 (d, 2H, pym-5), 9.83 (d, 2H, pym-2); UV/Vis (H_2O/DMSO 3:1): λ_{max} (ε) = 383 (9800), 543.5 nm (6700 $mol^{-1}dm^3cm^{-1}$); IR (KBr): $\tilde{\nu} = 2189$ (C≡N), 1102 (Cl–O), 625 (δ(Cl–O)) cm^{-1}; elemental analysis calcd (%) for $PdC_{30}H_{22}N_9ClO_6$ (746.4): C 48.27, H 2.97, N 16.89; found: C 47.88, H 2.75, N 16.86.

[(L–H)Cu$_3$][PO_4][ClO_4]$_2 \cdot 9H_2O$ (4): To a solution of [(L–H)Cu)]ClO_4 prepared as described above from ligand L (20 mg, 0.04 mmol), copper(II) perchlorate (0.1 M aqueous solution, 0.4 mL) and NaOH (0.04 mL 1 M

aqueous solution) in CH_2Cl_2/methanol (10/20 mL), two additional equivalents of $Cu(ClO_4)_2$ and then one equivalent aq Na_3PO_4 (0.1M, 0.2 mL) were added. The obtained deep blue solution was stirred 30 min at 40 °C, filtered, and saturated aqueous $NaClO_4$ was added (5 mL) to the filtrate. The precipitate was filtered off, washed with acetone, redissolved in methanol (30 mL) and then precipitated again by addition of diethyl ether (50 mL). The dark blue precipitate was separated by centrifugation and dried in vacuum (28 mg, 61 %). UV/Vis (DMSO): λ_{max} (ε) = 394 (19600), 587 nm (7000 $mol^{-1}dm^3cm^{-1}$); IR (KBr): $\tilde{\nu}$ = 2183 (C≡N), 1099 br (Cl−O, P−O), 625 (δ(Cl−O)) cm^{-1}; elemental analysis calcd (%) for $Cu_3C_{30}H_{36}N_9Cl_2PO_{21}$ (1151.2): C 31.30, H 3.15, N 10.95; found: C 31.26, H 2.98, N 10.80.

[(L−H)Cu$_2$]Cl$_3$·3H$_2$O (5): To a stirred solution of [(L−H)Cu)]Cl prepared as described above from ligand L (20 mg, 0.04 mmol), copper(II) chloride (0.1M in methanol, 0.4 mL) and aq LiOH (1M, 0.04 mL) in CH_2Cl_2/methanol (10/20 mL), two additional equivalents $CuCl_2$ were added at 40 °C. The blue-violet precipitate was separated by centrifugation, washed with acetone, diethyl ether, and dried in vacuo (23 mg, 73 %). UV/Vis (DMSO/MeOH 1:1): λ_{max} (ε) = 392 (26300), 534.5 nm (9000 $mol^{-1}dm^3cm^{-1}$); IR (KBr): $\tilde{\nu}$ = 2180 (C≡N), 3412 br (O−H) cm^{-1}; elemental analysis calcd (%) for $Cu_2C_{30}H_{24}N_9Cl_3O_4$ (799.0): C 45.49, H 3.05, N 15.92; found: C 45.39, H 3.17, N 15.76.

X-ray Crystallography: Details of the X-ray data collection and refinement for **1a** are given in Table 3.[34] Intensities were collected using a Bruker AXS CCD Smart 1000 diffractometer at 173 K. Corrections for Lorentz and polarization effects were applied. Absorption corrections were performed by semiempirical method based on multiple scans of equivalent reflections using SADABS routine.[35] The structure was solved by direct methods and refined by full-matrix, least-squares on all F_o^2 using SHELXTL NT V.5.1.[36] The non-hydrogen atoms were refined anisotropically. All the aromatic and O−H hydrogen atoms were localized in difference Fourier syntheses, and their positional and isotropic thermal parameters were included in the refinement. The methyl protons were included in calculated positions and allowed to ride on the atom to which they were linked.

Table 3. Crystal data and structure refinement for **1a**.[a]

empirical formula	$C_{31}H_{22}N_9O_5ClCu$
M_w	699.57
wavelength [Å]	0.71073
crystal system	monoclinic
space group	*C*2/*c*
a [Å]	22.070(2)
b [Å]	11.320(1)
c [Å]	23.876(2)
β [°]	110.972(2)
U [Å^3]	5569.9(7)
Z	8
ρ_{calcd} [$Mg\,m^{-3}$]	1.668
μ [mm^{-1}]	0.943
F(000)	2856
crystal size [mm]	0.26 × 0.14 × 0.06
θ range [°]	1.83 – 28.31
range *hkl*	−29 – 27, 0 – 15, 0 – 31
reflections collected	19274
independent reflections	6779
reflections with $I > 2\sigma(I)$	4787
data/parameters	6779/502
goodness-of-fit on F^2	1.033
final *R* indices [$I > 2\sigma(I)$]	$R1$[b] = 0.0511, $wR2$[c] = 0.1275
Final *R* indices (all data)	$R1$[b] = 0.0844, $wR2$[c] = 0.1517

[*a*] Weighting scheme applied $w = 1/\sigma^2(F_o^2) + (0.0729P)^2 + 17.16P$, where P is defined as $(F_0^2 + 2F_c^2)/3$. [b] $R1 = \Sigma(F_o - F_c)/\Sigma F_o$. [c] $wR2 = \{\Sigma[w(F_0^2 - F_c^2)^2]/\Sigma[w(F_0^2)^2]\}^{1/2}$.

Acknowledgement

This work was funded by the Deutsche Forschungsgemeinschaft (Gerhard Hess-Programm)and supported by the Fonds der Chemischen Industrie.

[1] E. E. Kim, H. W. Wyckoff, *J. Mol. Biol.* **1991**, *218*, 449.
[2] a) G. Cathala, C. Brunel, D. Chappelet-Tordo, M. Lazdunski, *J. Biol. Chem.* **1975**, *250*, 6046; b) G. Linden, D. Chappelet-Tordo, M. Lazdunski, *Biochem. Biophys. Acta* **1977**, *483*, 100.
[3] J. E. Murphy, T. T. Tibbits, E. R. Kantrowitz, *J. Mol. Biol.* **1995**, *253*, 604.
[4] T. Nabeshima, *Coord. Chem. Rev.* **1996**, *148*, 151.
[5] R. Baldes, H.-J. Schneider, *Angew. Chem.* **1995**, *107*, 380; *Angew. Chem. Int. Ed. Engl.* **1995**, *34*, 321.
[6] A. Ikeda, Y. Suzuki, M. Yoshimura. S. Shinkai, *Tetrahedron* **1998**, *54*, 2497.
[7] Y. Kubo, Y. Murai, J.-I. Yamanaka, S. Tokita, Y. Ishimaru, *Tetrahedron Lett.* **1999**, *40*, 6019.
[8] For further examples on negative allostery, see: M. H. Al-Sayah, N. R. Branda, *Angew. Chem.* **2000**, *112*, 975; *Angew. Chem. Int. Ed.* **2000**, *39*, 945; and references therein.
[9] F. Wang, A. W. Schwabacher, *J. Org. Chem.* **1999**, *64*, 8922.
[10] a) O. S. Tee, M. Bozzi, N. Clement, T. A. Gadosy, *J. Org. Chem.* **1995**, *60*, 3509; b) O. S. Tee, M. Bozzi, J. J. Hoeven, T. A. Gadosy, *J. Am. Chem. Soc.* **1993**, *115*, 8990.
[11] E. Iglesias, *J. Am. Chem. Soc.* **1998**, *120*, 13057.
[12] a) J. Rebek, Jr., T. Costello, R. Wattley, *J. Am. Chem. Soc.* **1985**, *107*, 7487; b) J. Rebek, Jr., *Acc. Chem. Res.* **1984**, *17*, 258.
[13] I. O. Fritsky, R. Ott, R. Krämer, *Angew. Chem.* **2000**, *112*, 3403; *Angew. Chem. Int. Ed.* **2000**, *39*, 3255.
[14] R. Krämer, I. O. Fritsky, *Eur. J. Org. Chem.* **2000**, 3505.
[15] E. Bejan, H. A. Aït-Haddou, J.-C. Daran, G. G. A. Balavoine, *Synthesis* **1996**, 1012.
[16] J. E. Parks, B. E. Wagner, R. H. Holm, *J. Organomet. Chem.* **1973**, *56*, 53.
[17] A. L. Borror, A. F. Haeberer, *J. Org. Chem.* **1965**, *30*, 243.
[18] S. Ogawa, R. Narushima, Y. Arai, *J. Am. Chem. Soc.* **1984**, *106*, 5760.
[19] F. A. Walker, E. Hui, J. M. Walker, *J. Am. Chem. Soc.* **1975**, *97*, 2390.
[20] a) A. MacCragh, C. B. Storm, W. S. Koski, *J. Am. Chem. Soc.* **1965**, *87*, 1470; b) K. L. Cunningham, K. M. McNett, R. A. Pierce, K. A. Davis, H. H. Harris, D. M. Falck, D. R. McMillin, *Inorg. Chem.* **1997**, *36*, 608.
[21] J. Peisach, W. E. Blumberg, *Arch. Biochem. Biophys.* **1974**, *165*, 691.
[22] M. Wicholas, R. S. Drago, *J. Am. Chem. Soc.* **1968**, *90*, 6946.
[23] a) H. Gornitzka, D. Stalke, *Angew. Chem.* **1994**, *106*, 695; *Angew. Chem. Int. Ed. Engl.* **1994**, *33*, 693; b) H. Gornitzka, D. Stalke, *Organometallics* **1994**, *13*, 4398.
[24] S. C. Nyburg, C. H. Faerman, L. Prasad, *Acta Crystallogr. Sect. B* **1987**, *43*, 106.
[25] a) J. R. Morrow, W. C. Trogler, *Inorg. Chem.* **1988**, *27*, 3387; b) R. L. Gustafson, A. E. Martell, *J. Am. Chem. Soc.* **1959**, *81*, 525.
[26] Inhibition of HPNP cleavage by excess Cu which binds to the catalyst via bridging hydroxides is a possible explanation of this effect, compare E. Kövari, J. Heitker, R. Krämer, *J. Chem. Soc. Chem. Commun.* **1995**, 1205.
[27] a) R.Krämer, T. Gajda in *Perspectives on Bioinorganic Chemistry*, *Vol. 4* (Eds.: R. W. Hay, J. R. Dilworth, K. B. Nolan), JAI Press, **1999**, pp. 209 – 240; b) N. H. Williams, B. Takasaki, J. Chin, *Acc. Chem. Res.* **1999**, *32*, 485; c) P. Molenveld, J. F. J. Engbersen, D. N. Reinhoudt, *Chem. Soc. Rev.* **2000**, *29*, 75.
[28] a) M. Wall, R. C. Hynes, J. Chin, *Angew. Chem.* **1993**, *105*, 1696; *Angew. Chem. Int. Ed. Engl.* **1993**, *32*, 1633; b) S. Liu, A. D. Hamilton, *Bioorg. Med. Chem. Lett.* **1997**, *7*, 1785; c) P. Molenveld, J. F. J. Engbersen, H. Kooijmann, A. L. Spek, D. N. Reinhoudt, *J. Am. Chem. Soc.* **1998**, *120*, 6726.
[29] T. Gajda, R. Krämer, A. Jancsó, *Eur. J. Inorg. Chem.* **2000**, 1635.
[30] J. R. Morrow, L. A. Buttrey, K. A. Berback, *Inorg. Chem.* **1992**, *31*, 16.
[31] H. Sigel, *Angew. Chem.* **1975**, *87*, 391; *Angew. Chem. Int. Ed. Engl.* **1975**, *14*, 394.
[32] a) W. H. Chapman, Jr., R. Breslow, *J. Am. Chem. Soc.* **1995**, *117*, 5462; b) F. Meyer, E. Kaifer, P. Kircher, K. Hienze, H. Pritzkow, *Chem. Eur. J.* **1999**, *5*, 1617.

  0947-6539/01/0706-1230 $ 17.50+.50/0

[33] D. M. Brown, D. A. Usher, *J. Chem. Soc.* **1965**, 6558.
[34] Crystallographic data (excluding structure factors) for the structure reported in this paper have been deposited with the Cambridge Crystallographic Data Centre as supplementary publication no. CCDC148135. Copies of the data can be obtained free of charge on application to CCDC, 12 Union Road, Cambridge CB2 1EZ, UK (fax: (+44) 1223-336-033; e-mail: deposit@ccdc.cam.ac.uk).
[35] G. M. Sheldrick, *SADABS*, *Program for Scaling and Correction of Area Detector Data*, University of Göttingen, Germany, **1996**.
[36] G. M. Sheldrick, *SHELXTL*, Version NT V5.1., Bruker AXS, Madison, Wisconsin, USA, **1998**.

Received: August 10, 2000 [F2666]